Landscape and Urban Planning 152 (2016) 59–71

Contents lists available at ScienceDirect

Landscape and Urban Planning

journal homepage: www.elsevier.com/locate/landurbplan

Research paper

Capturing the varying effects of driving forces over time for the simulation of urban growth by using survival analysis and cellular automata

Yimin Chen [a], Xia Li [a,*], Xiaoping Liu [a], Bin Ai [b], Shaoying Li [c]

[a] Guangdong Provincial Key Laboratory of Urbanization and Geo-simulation, School of Geography and Planning, Sun Yat-sen University, Guangzhou, PR China
[b] School of Marine Sciences, Sun Yat-sen University, Guangzhou, China, PR China
[c] School of Geographical Sciences, Guangzhou University, Guangzhou, PR China

HIGHLIGHTS

- The temporal adaptation of CA is enhanced through survival analysis.
- Simulation accuracy is improved by using a patch-based simulation strategy.
- Urban growth in Shenzhen is simulated and predicted.

ARTICLE INFO

Article history:
Received 11 March 2015
Received in revised form 7 March 2016
Accepted 19 March 2016

Keywords:
SA-Patch-CA
Survival analysis
Patch-based simulation
Strategy
Urban growth simulation

ABSTRACT

Cellular automata (CA) have been widely used for simulating realistic urban growth. With the increasing availability of multitemporal land-use data, there remains challenges in how to effectively utilize these data for calibrating CA models. Most of existing calibration methods, such as logistic regression, lack the ability to unveil the temporal dynamics that is encapsulated in the multi-temporal land-use data. This study aims to enhance the temporal adaptation of CA models by using the approach of survival analysis (SA). SA can capture the time-dependent influences of driving factors from a time-series of land-use data. Thus, SA has substantial potential to facilitate the calibration of CA models and consequently improve the simulation performance. Moreover, a patch-based simulation strategy is integrated into the proposed model (SA-Patch-CA) to produce more realistic simulated patterns. The proposed SA-Patch-CA was tested and compared with another two recently developed CA models, namely Logistic-Patch-CA and LEI-CA, through the experiments of urban growth simulation in Shenzhen, China, during the period of 1990–2012. The simulated patterns of these models were validated at cell- and pattern-level. The results revealed that the proposed SA-Patch-CA outperforms Logistic-Patch-CA with the better cell level accuracy and pattern-level similarity, and also avoids the 'saltand- pepper' effect which was found to be the major weakness of LEI-CA. The proposed SA-Patch-CA were also used to conduct scenario analysis of future development of Shenzhen from 2012 to 2018. Such simulation experiments are useful in that they allow decision makers to assess the outcomes and impacts of different policies.

1. Introduction

Urban land-use change modeling has drawn increased attention from different academic fields as the expanding cities in the world have caused many irreversible impacts on the global biosphere (Seto, Fragkias, Güneralp, & Reilly, 2011). Simulation is an important approach to investigate the evolution of urban systems (Clarke, 2014). Perhaps cellular automata (CA) have now become the most popular urban simulation models among others (Santé, García, Miranda, & Crecente, 2010). Various kinds of urban CA models have been developed over the past two decades for simulating real urbanization processes (Aljoufie, Zuidgeest, Brussel, van Vliet, & van Maarseveen, 2013; Clarke & Gaydos, 1998; He, Zhao, Tian, & Shi, 2013; Li & Yeh, 2004; Wang & Marceau, 2013; Liu, Li, Liu, He, &

* Corresponding author at: School of Geography and Planning, Sun Yat-sen University, 135 West Xingang RD, Guangzhou 510275, PR China.
E-mail addresses: lixia@mail.sysu.edu.cn, lixia@graduate.hku.hk (X. Li).
URL: http://www.geosimulation.cn/ (X. Li).

http://dx.doi.org/10.1016/j.landurbplan.2016.03.011
0169-2046/

Ai, 2008). The application of CA models often requires proper calibration. A problem with many contemporary calibration methods, such as logistic regression (Wu, 2002), artificial neural networks (Basse, Omrani, Charif, Gerber, & Bódis, 2014; Li & Yeh, 2002), support vector machine (Samardžić-Petrović, Dragićević, Kovačević, & Bajat, 2015) and data mining (Li & Yeh, 2004; Omrani, Abdallah, Charif, & Longford, 2015; Tayyebi & Pijanowski, 2014), is that they often use only two sets of land-use data for calibration (i.e. data at the beginning and the end of the study period, respectively). Although these methods can capture the spatial complexities well, they fail to address the temporal complexities and the implicit dynamic information of land-use change (An & Brown, 2008).

The SLEUTH model can be considered as an exception (Clarke & Gaydos, 1998), because it involves a time-series of land-use data for calibration. However, the SLEUTH model uses an exhaustive search method that makes the calibration procedure extremely time-consuming. This would be even worse if data with fine spatial resolution were used. Recently, Liu et al. (2014) developed LEI-CA by integrating the landscape expansion index (LEI) (Liu et al., 2010) into a CA model. This model employs a case-based reasoning (CBR) approach to simulate the land-use conversion from non-urban to urban. Such an approach can implicitly derive the spatial-temporal dynamics of land-use change through a built-in library, which is composed of known cases (training data) collected from different locations and periods. This model can also simulate spontaneous growth that is not always explicitly addressed by conventional CA models.

In this study, we demonstrated the use of an alternative method, survival analysis (SA), to incorporate CA models with the temporal variations of urban dynamics derived from a time-series of land-use data. SA is a group of statistical methods that most often deals with the events of deaths in biological or medical fields. SA is also useful for investigating other kinds of events such as accidents, machine failures, or crimes (Allison, 2012). However, applications of SA in land-use change modeling are rare until quite recently (An & Brown, 2008; An, Brown, Nassauer, & Low, 2011; Greenberg, Kefauver, Stimson, Yeaton, & Ustin, 2005). An and Brown (2008) pointed out that traditional statistical methods for land-use change studies, such as logistic regression models and multivariate linear regression models, are short at predicting the temporal variations of the key driving factors. Such a limitation can affect the simulation accuracy if these methods are used to calibrate CA models. In fact, the temporal aspects should not be left out when simulating the evolution of land-use patterns. This can be better addressed through SA which is able to reflect the varying effects of driving forces over time. Literature also revealed that SA outperforms logistic regression (Wang, Brown, An, Yang, & Ligmann-Zielinska, 2013), a method which has been applied to the calibration of CA models (Wu, 2002). Compared with the exhaustive search method, SA is apparently a much more efficient approach to analyze time-series land-use data.

Moreover, conventional urban CA models usually adopt a cell-based simulation strategy, but it has several drawbacks that might affect the simulation performance: 1) The assumption that a regular cell represents the basic unit of land-use entity is not always reasonable, especially when high-resolution data are involved (Wang & Marceau, 2013). 2) Unexpected bias might exist if the cell-based simulation strategy is applied, such as the "salt-and-pepper" effect (Wu, 2002), or the failure of simulating spontaneous urban growth for some models (García, Santé, Boullón, & Crecente, 2012). 3) There is a risk of overfitting when using the cell-based simulation strategy. It is extremely difficult to precisely predict the location of land-use change at the cell-level because land-use change in the real world is characterized by stochasticity and path-dependences. However, if the model was forced to produce simulations in which the locations (cells) of land-use change are strictly match the referenced data, then this model would inevitably have poor generalization and prediction abilities (Brown, Page, Riolo, Zellner, & Rand, 2005).

To address these issues, two kinds of approaches have been proposed in the literature. The first one is to thoroughly change the formal structure of CA by using vector/irregular cells instead of regular cells. Apparently the vector/irregular structure can better represent the realistic land surfaces which consist of parcels with different size and shape. There have been several studies that deal with the development of vector-based or irregular CA models (Moreno, Ménard, & Marceau, 2008; Moreno, Wang, & Marceau, 2009; Stevens, Dragicevic, & Rothley, 2007). However, the research of these new kind of CA models is still in its infancy, and the major problems exist in the definition of neighborhood, the representation of interactions and also the computation bottlenecks (Barreira-González, Gómez-Delgado, & Aguilera-Benavente, 2015). The second approach to overcome the drawbacks of cell-based simulation is the incorporation of the patch structure into conventional CA models. Recent studies have demonstrated that the patch-based CA models perform better than the cell-based models in replicating realistic urban land-use patterns (Chen, Li, Liu, & Ai, 2014; Meentemeyer et al., 2013; Wang & Marceau, 2013). These models are appealing also because conventional CA models can be easily adapted into the patch-based model due to the inherent connection between cells and patches (i.e. cells form patches). Therefore, in this study we integrated a patch-based simulation strategy (Chen et al., 2014) into the proposed model for obtaining a more realistic urban growth patterns. This integrated model is referred to as SA-Patch-CA below.

The proposed model will be implemented to simulate the urban growth in Shenzhen during 1990–2012. Two recently developed models of Logistic-Patch-CA (Chen et al., 2014) and LEI-CA (Liu et al., 2014) are also run for making a comparative analysis. The results of these three models are validated and compared at both cell-level and pattern-level using the indicator of 'Figure of merit' and a set of landscape metrics. Finally, the proposed SA-Patch-CA is used to perform scenario simulations of future developments of Shenzhen from 2012 to 2018.

2. Study area and data

Shenzhen is located in the mouth of the Pearl River Delta next to Hong Kong (Fig. 1). Shenzhen used to be a small fishing village with less than 20,000 people. However, it rapidly grew into a megacity with a recent population of more than 10 million after the designation of the special economic zone (SEZ) by the central government of China in 1979. Besides the favorable development policies for the SEZ (e.g. tax relief and low land rent), the spatial proximity and the tight social links to Hong Kong also helped Shenzhen to attract a tremendous amount of domestic and foreign investments (Sui & Zeng, 2001). However, the rapid urbanization in Shenzhen has caused many negative impacts, such as loss of arable land (Seto et al., 2002), degradation of natural environments (Güneralp & Seto, 2008), increasing demand of energy resources (Chen, Li, Wang, Liu, & Ai, 2013), and problems of social inequity (Ng, 2003). Urban simulation, especially the modeling of land-use conversion, can provide useful knowledge and technical support to cope with various problems resulted from fast urbanization (Clarke, 2014).

The urban land-use data were derived from 14 scenes of classified Landsat images (122–44 and 121–44) in the years of 1990, 1995, 2000, 2003, 2006, 2009 and 2012 with a 30-m resolution (Fig. 2). The land-use classifications were validated based on field survey. The classification accuracies of the urban land-use for each year are 91.03% (1990), 92.68% (1995), 91.36% (2000), 92.10% (2003), 94.81% (2006), 95.77% (2009) and 97.29% (2012).

Fig. 1. Geographical location of Shenzhen city and its district centers.

A group of spatial variables for the implementation of SA-Patch-CA were generated by using common GIS functions. These variables include: (1) proximity to town/city centers; (2) proximity to transportation network/hubs (e.g. the airport, highways, major roads, railway stations and ports); (3) physical conditions (e.g. slope) of a site for development. The proximity variables are expressed as the distance from cells to the nearest transportation network/hubs, and these variables are generated based on the transportation layers in each of the years 1995, 2000, 2003, 2006, 2009 and 2012. To obtain these layers, we used the 2012 transportation layer as the reference data, and overlapped it with the Landsat images so that the 'inexistent' entities (e.g. roads/highways) in the years of 2009, 2006, 2003, 2000 and 1995 could be identified. By subtracting the 'inexistent' entities correspondingly from the 2012 layer, the transportation layers can then be produced for each of the remaining years. The variables of proximity to town/city centers and slope were held unchanged because these conditions were relatively stable during the study periods. Fig. 3 shows these input variables in the year of 2006 as an example. All of these numeric variables were normalized into [0,1]. The spatial resolution of these variables is 30 m, which is also the cell size for implementing the subsequent simulations.

3. Urban growth simulation using SA-Patch-CA

Fig. 4 depicts the procedure of urban growth simulation using the proposed SA-Patch-CA. First, land-use data of multiple years are used to collect cell samples and to derive the area distributions of new urban patches for each period (Fig. 2). Second, the sampled cells will go through the censoring procedure to generate the censored data as required by the approach of SA. Third, the censored data are used to calibrate the CA model based on SA. Fourth, urban growth simulation is carried out by using a patch-based

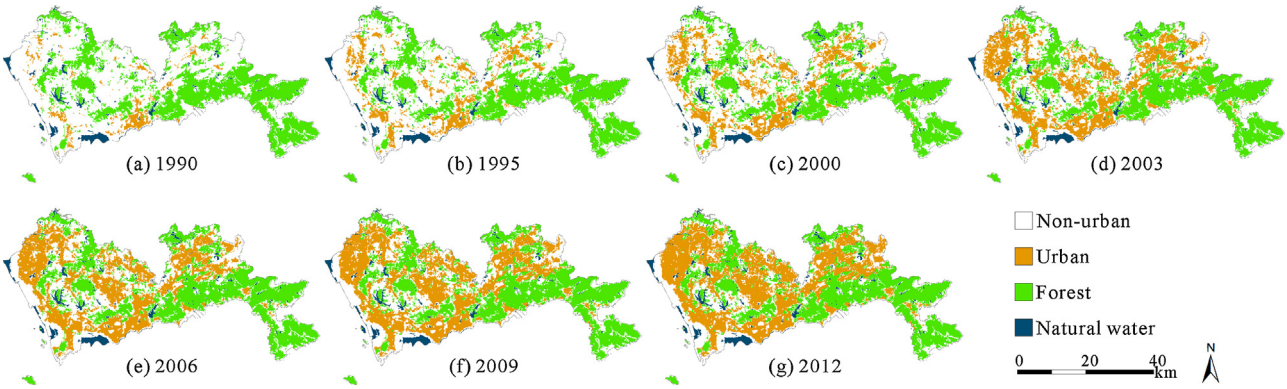

Fig. 2. Land-use data of Shenzhen for the simulation of urban expansion.

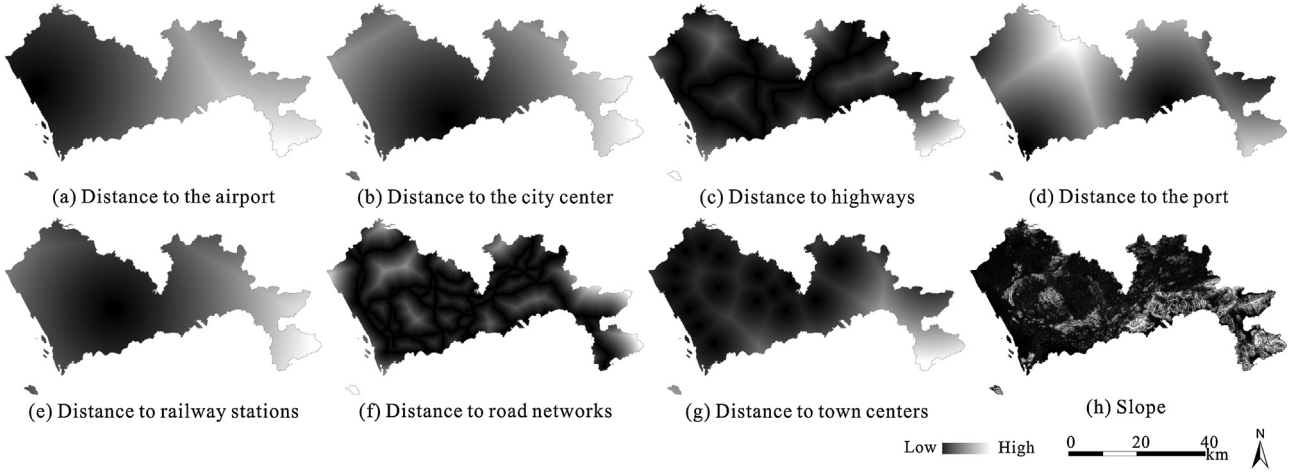

Fig. 3. Various spatial variables for the implementation of SA-Patch-CA (data in 2006 as an example): (a) Distance to the airport; (b) distance to the city center; (c) distance to highways; (d) distance to the port; (e) distance to railway stations; (f) distance to road networks; (g) distance to town centers; (h) slope.

simulation strategy with the calibrated parameters and the observed area distributions. More details of the specifications of SA and the patch-based simulation strategy are described in Sections 3.1 and 3.2.

3.1. Model calibration through survival analysis

Originally SA is used to study the mortality of individuals, such as patients or animals. For many other disciplines, including land change science (An & Brown, 2008), SA can be employed to investigate the occurrence and timing of events for a specific period (e.g. land-use change). In the analysis of urban growth, the event of interest for a land unit (e.g. a cell) is its state conversion from non-urban to urban, which is analogous to an individual's death. Then the survival time for a non-urban cell is the time duration to until its state conversion occurs.

In SA, the probability of an individual survivals over time t is described using the survival function $S(t)$:

$$S(t) = Pr(T > t) \tag{1}$$

where T is the event time. Generally $S(0)$ should be 1; while $S(t) = 0$ $(t \to \infty)$. The derivative of $S(t)$, which is an equivalent way of describing the probability distribution, is called the hazard function (Allison, 2012):

$$h(t) = \lim_{\Delta t \to 0} \frac{Pr(t \le T < t + \Delta t | T \ge t)}{\Delta t} = -\frac{d}{dt} \log S(t) \tag{2}$$

where $h(t)$ represents the risks that an event will happen in the small interval between t and $t + \Delta t$ $(\Delta t \to 0)$ given that the individual survives to time t. In the context of urban land-use conversion, $h(t)$ can be interpreted as the development potential of a non-urban cell being developed in the small interval between t and $t + \Delta t$ $(\Delta t \to 0)$ conditional on that cell remains non-urban to time t.

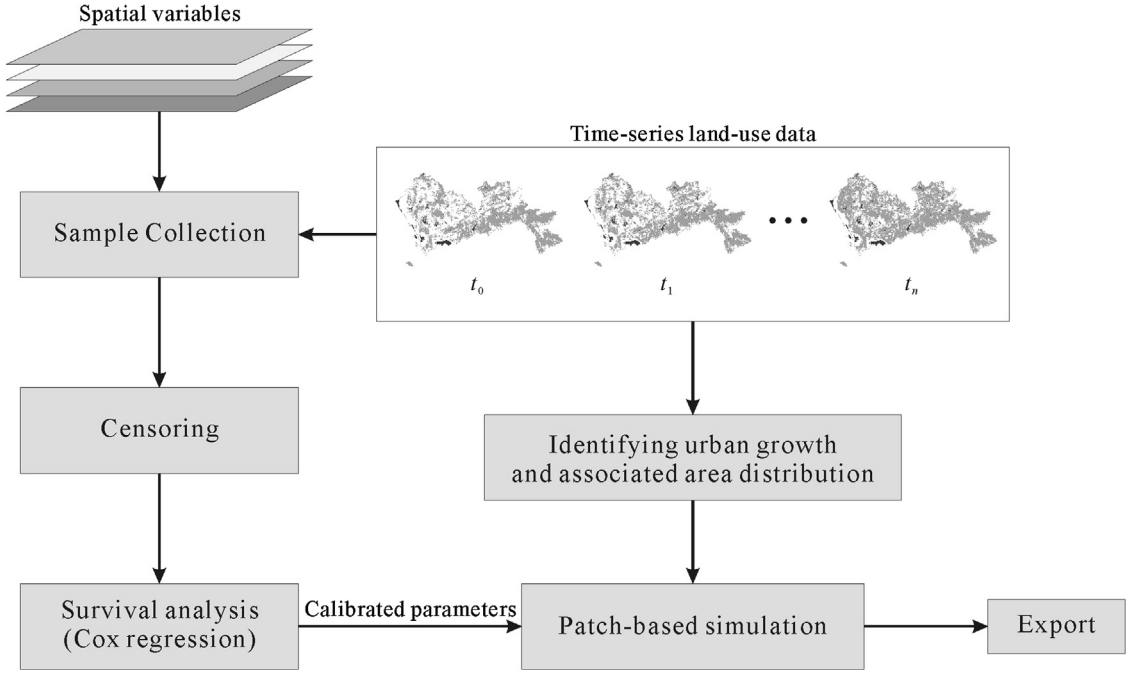

Fig. 4. The integration of SA and a patch-based CA for simulating urban growth.

Table 1
Examples of right censored and interval censored observations.

Cell ID	Start time	End time	Period	State	x_1	x_2	x_3	x_4
A	1990	1995	1	0	0.001	0.002	0.013	0.500
A	1995	2000	2	0	0.024	0.036	0.013	0.500
A	2000	2006	3	0	0.024	0.076	0.013	0.510
B	1990	1995	1	0	0.402	0.032	0.033	0.790
B	1995	2000	2	1	0.355	0.011	0.028	0.790

Note: State 0 represents non-urban, and 1 represents urban. $x1$–$x4$ are independent variables.

SA requires observations to be censored. The forms of censored observations depend on whether and when the individual experiences the event (e.g. death or change of states). For example, given that the study period is $[t_0, t_n]$, if a cell was developed at before t_0, it is a left censored observation; if it remains non-urban after t_n, this cell is a right censored observation; otherwise, if this cell is developed during the period between t_0 and t_n, it becomes an interval censored observation. Table 1 provides some examples of the right censored and interval censored observations. Most often, researchers are more interested in the occurrence of the event as well as its relation with time, therefore only interval/right censored observations are used while left censored observations are eliminated from the sample data.

In some applications, the time variable t is continuous, which means when the event occurred is exactly known. However, in the context of land-use change it is almost impossible to know the precise time at which the land-use conversions occur. In this case, the entire time frame can be discretized into several periods (Table 1). Then $h(t)$ can be understood as the average risks that a cell would be subject to over time (An & Brown, 2008). As shown in Table 1, each cell has a record for each period unless the state of the cell changes. It can be seen that cell A is non-urban throughout the periods of 1–3, thus it has three records and is labeled as a right censored observation; while cell B is non-urban in period 1 but becomes urban in period 2, thus it has only two records and is labeled as an interval censored observation.

After all observations (sampled cells) are censored, they can be used to estimate the $h(t)$ in Eq. (2). In this study, the risks $h(t)$ is used to represent the development potential of the non-urban cells for development. The calculation of $h(t)$ is based on the frequently used Cox regression model (Cox, 1972):

$$h_i(t) = \lambda_0(t)\exp(\beta_1 x_{i1} + \beta'_1 x_{i1}(t) \ldots + \beta_k x_{ik} + \beta'_k x_{ik}(t)) \quad (3)$$

Taking the logarithm of both sides, Eq. (3) can be rewritten as:

$$\log h_i(t) = \alpha(t) + \beta_1 x_{i1} + \beta'_1 x_{i1}(t) \ldots + \beta_k x_{ik} + \beta'_k x_{ik}(t) \quad (4)$$

where $h_i(t)$ is the development potential of cell i at time t; $\lambda_0(t)$ is the baseline hazard function and can be left unspecified (actually it can take any form except that it cannot be negative) (An & Brown, 2008); x_{ik} are a set of spatial variables (e.g. proximity to city centers, Fig. 3), and $x_{ik}(t) = x_{ik} \times t$ which represents the time-dependent effects of each x_{ik} (Allison, 2012). Whether to place the time-dependent variables in the model depends on the correlation analysis between the Schoenfeld residuals and the time variable t. For example, if the correlation is significant between x_{i1}'s Schoenfeld residuals and the time variable t, then $x_{i1}(t)$ should be added into the model. The detailed calculation of the Schoenfeld residuals can be found in (Allison, 2012). Afterward, the coefficients of β_k and $\beta_{k'}$ are estimated using the method of partial likelihood, which can be easily accomplished through the statistical package SAS (Statistical Analysis System; http://www.sas.com/en_us/home.html).

In addition to the development potential $h_i(t)$, the neighborhood development density, denoted as $\Omega^t{}_i$, is also considered to represent the effect of positive feedback in realistic urban development processes:

$$\Omega_i^t = \frac{\sum_{n^2} con(s_i = developed)}{n^2 - 1} \quad (5)$$

where $con()$ returns 1 if the state of cell i is developed, otherwise returns 0; $\sum_{n^2} con(s_i = developed)$calculates the number of developed cells in a $n \times n$ Moore neighborhood ($n = 3$). The choice of the form of neighborhood could influence the simulation outcomes. Kocabas and Dragicevic (2006) conducted comprehensive experiments to assess the sensitivity of simulation outcomes with respect to neighborhood types. They found increasing discordance between simulations after changing the sizes and types of neighborhoods. Nevertheless, the Moore neighborhood is used in this study primarily because it is the main stream neighborhood configuration for urban simulations as reviewed by Santé et al. (2010). Additionally, as our focus is to assess and compare the performance of the proposed model against others, the same neighborhood configuration is also adopted in another two models of Logistic-Patch-CA and LEI-CA (see Section 4.2). It is expected that the influences, if exist, could be minor on the interpretation of variations in the outcomes from different models with the same Moore neighborhood. Overall, the development probability $p_i{}^t$ is formulated as:

$$p_i^t = h_i(t)\Omega_i^t con(s_i = suitable) \quad (6)$$

where $con()$ returns 1 if cell i is not of natural water or protected forest.

3.2. Patch-based simulation strategy

The patch-based simulation strategy adopted in this study was designed by Chen et al. (2014). It is an iteration method that produces only one simulated new patch at each iteration (Fig. 5(a)). For the simulation of the entire urban growth process, the production of patches will be iteratively run until the total area of simulated patches matches the predefined areal constraint.

Before running this strategy, the observed area distribution of new urban patches should be obtained from empirical land-use data. Then this distribution will be used to estimate the size of the simulated patches (i.e. the number of cells). Specifically, the size of a new patch is determined at the beginning of each iteration through a power function (Chen et al., 2014; Fragkias & Seto, 2009):

$$A_i = a_0(r_{area})^{a_1} \quad (7)$$

where A_i is the size of patch i; r_{area} is a random variable within (0, 1]; a_0 and a_1 are parameters calibrated with the following steps: 1) identifying the new urban patches in each period (e.g. 1990–1995) and sorting them in descending order by patch size; 2) for each period, deriving the proportions for each patch size and calculate the respective cumulative proportion; and 3) estimating a_0 and a_1 by fitting the cumulative proportions using Eq. (7).Then the new patch will be categorized either as spontaneous growth or organic growth. Here the spontaneous growth, which is also referred to as leapfrog growth, means that new urban patches disconnect from the initial urban areas, while the organic growth represents the self-expansion of the initial urban areas (Fig. 5(b)). The growth type of the new patch is defined by comparing the value of a random pointer r_{type} and the pre-defined threshold T_{spon}. If r_{type} is less than T_{spon}, then the new patch is defined as spontaneous growth; otherwise it is organic growth. The parameter T_{spon} can be tuned through a trial-and-error approach.

The simulation of patch growth is carried out in two steps. First, the location of the very first developed cell of the new patch, i.e. the

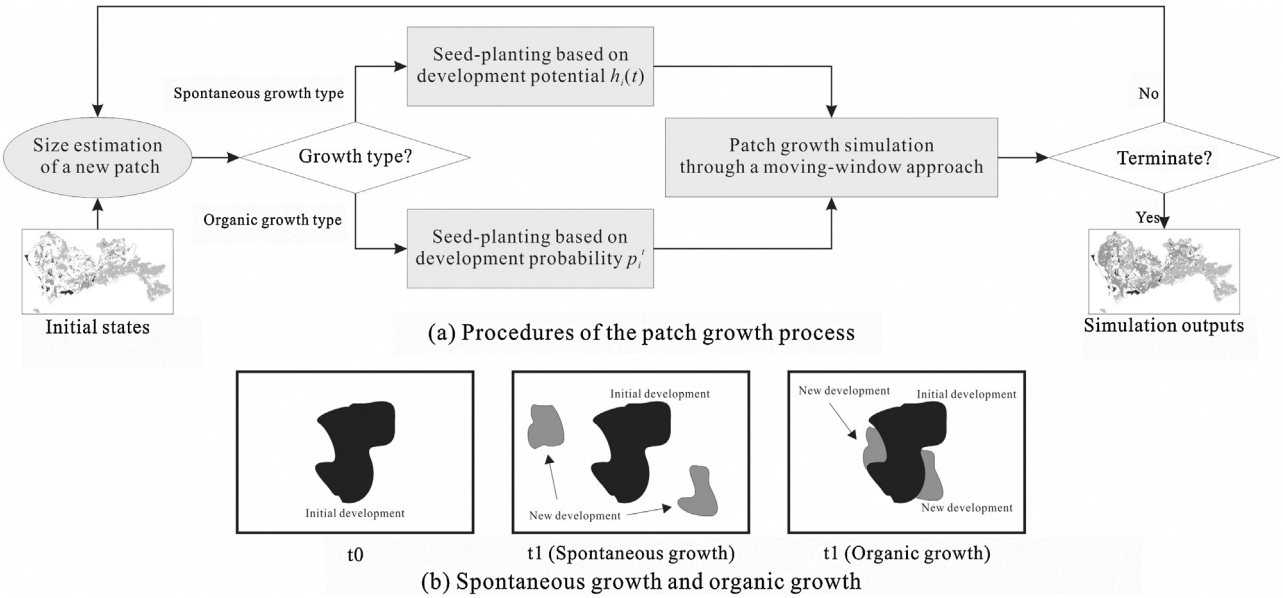

Fig. 5. (a) Urban growth simulation by iteratively implementing the patch growth process; (b) examples of two urban growth types: spontaneous growth and organic growth.

seed, should be determined. Second, subsequent developments will spread out from the seed. Specifically, for patches that are of spontaneous growth type, a non-urban cell is first randomly picked, and then its development potential $h_i(t)$ (Eq. (3)) is compared with a random value within [0,1]: if $h_i(t)$ is larger, the selected non-urban cell becomes the seed and its state changes into urban; otherwise another non-urban cell will be picked and evaluated again until the seed is settled. For patches that are of organic growth type, the seed allocation follows the same procedures described above except that the development probability p_i^t (Eq. (6)) instead of $h_i(t)$ is used when evaluating the randomly picked non-urban cells. After that the remaining cells of the new patch is allocated into the space through a 3×3 moving-window (Fig. 6). The window first centers on the seed (Fig. 6(a)). Then one of the non-urban cells in this window is picked for the next development based on the approach of roulette wheel selection using the values of p_i^t (Fig. 6(b)). Afterward, the new developed cell becomes the center of the window and another non-urban cell is selected for development through the same approach (Fig. 6(c)). Such procedures continue (Fig. 6(d)) until the estimated patch size (Eq. (7)) is reached or the non-urban cells within the window are depleted.

4. Model implementation and results

4.1. Calibration

The land-use data of years 1990, 1995, 2000 and 2006 were used for calibration, while the others (i.e. 2003, 2009 and 2012) were regarded as the reference data for evaluating the prediction accuracy of the proposed model. The land-use data for calibration were overlapped so that the changing states for any cell could be coded as a chain. Some examples are given below:

#1: 0111 = > non-urban in 1990; urban in 1995, 2000 and 2006;

#2: 0011 = > non-urban in 1990 and 1995; urban in 2000 and 2006;

#3: 0000 = > non-urban throughout all periods; and

#4: 1111 = > already urban in 1990.

As aforementioned, only the interval censored and right censored observations (i.e. #1-2 and #3) were used to calibrate the model, whereas the left censored observations (i.e. #4) were excluded. Therefore, we randomly drew a total of 20% of the interval censored and right censored cells with their attributes (i.e. proximity to town/city centers, transportation network/hubs, and slope) in respective years to form the calibration dataset.

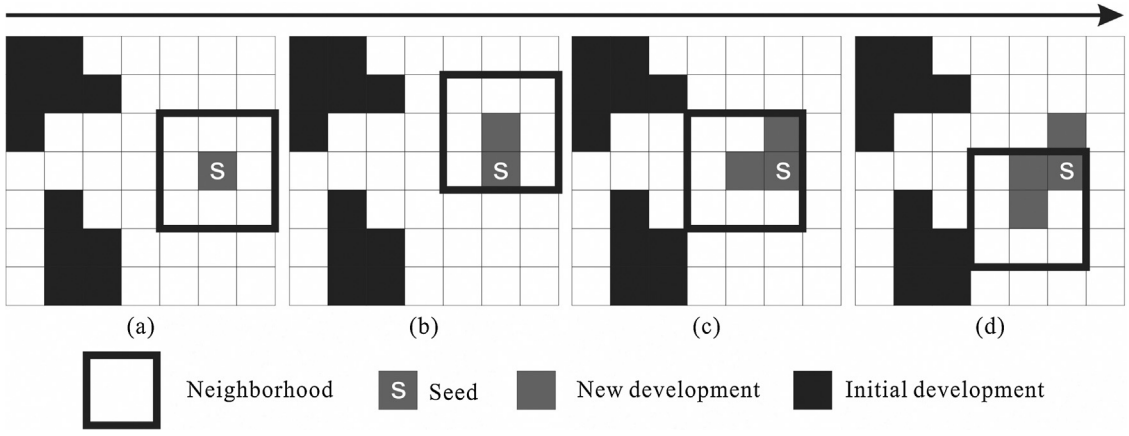

Fig. 6. Simulating patch growth through a moving-window approach.

Table 2
Correlation between the Schoenfeld residuals and the time variable t.

$x_{citycenter}$	$x_{towncenter}$	$x_{railstat}$	x_{port}	$x_{airport}$	$x_{express}$	x_{mroad}	x_{slope}
−0.017	−0.003	−0.106*	0.189***	−0.199***	0.094	0.157**	−0.007

Note: * Significant at 0.05; ** Significant at 0.01; *** Significant at 0.001.

Table 3
Results of the Cox regression and the calibrated T_{spon}.

$x_{citycenter}$	$x_{towncenter}$	$x_{railstat}$	x_{port}	$x_{airport}$	$x_{express}$	x_{mroad}	x_{slope}
4.208	−1.009	−4.837	−9.862*	6.029**	−2.858*	−11.325***	−9.438***

$x_{railstat}(t)$	$x_{port}(t)$	$x_{airport}(t)$	$x_{express}(t)$	T_{spon}
−0.010	0.785**	−0.404**	0.552**	0.0057

Note: * Significant at 0.05; ** Significant at 0.01; *** Significant at 0.001.

Table 4
The calibrated parameters of a_0 and a_1.

Periods	1990–1995	1995–2000	2000–2006	2006–2012
a_0	20.65	19.50	17.02	14.39
a_1	−1.14	−0.98	−1.20	−1.03

With this dataset, a correlation analysis was then performed between the Schoenfeld residuals of spatial variables and the time variable t to identify which of them needs the extra term of $x_{ik}(t)$. As a result, the Schoenfeld residuals of $x_{railstat}$, x_{port}, $x_{airport}$ and x_{mroad} are significantly correlated with the time variable t (Table 2). Thus, extra terms of $x_{railstat}(t)$, $x_{port}(t)$, $x_{airport}(t)$ and $x_{mroad}(t)$ were included in the model. Then the partial likelihood method was implemented to estimate the coefficients of β_k and β_k', which are shown in Tables 3 and 4. The variables of $x_{citycenter}$, $x_{towncenter}$, $x_{railstat}$, and $x_{railstat}(t)$ are not used in the subsequent calculation of $h_i(t)$ as their coefficients are not significant.

The parameters listed in Table 3 reflect the urban signatures of Shenzhen and its temporal variations from 1990 to 2006. The coefficients of the distance variables $x_{express}$ and x_{mroad} are negative and significant. This indicates an intense attraction effect of the road networks for new urban development. Fig. 2 also reveals that many urban patches stretch throughout the landscape along the road networks and form a disperse land-use pattern. Moreover, the positive coefficient of $x_{express}(t)$ suggests an increasing attraction effect of expressway over time. Such a spatial relationship between urban growth and transportation network was related to the fast industrialization in Shenzhen, and also has been termed as 'desakota' by previous literature (Sui & Zeng, 2001). As a vast number of the new urbanized areas are built for industrial uses, they are more likely to appear near the road networks to smooth the import/export of raw materials and products. In fact, the advantageous transportation convenience was one of the crucial factors that favored the developments of Shenzhen at its initial stages by facilitating the influx of capitals from Hong Kong to Shenzhen (Hou & Li, 2011). Even in today, the transportation network of Shenzhen is an important part of the provincial government's plan to fulfill the strategic aim of "building the world-class city cluster in the Pearl River Delta" (Shin, 2014). In addition, the coefficients of x_{port} and $x_{port}(t)$ imply that land with shorter distance to the port are more likely to be developed, and this trend is also enhancing over time. This is consistent with the intention of building the Yantian Port in east Shenzhen with the goal to maintain the city's competitiveness in attracting foreign investments and develop an export-oriented economy since early 1990s (Ng & Xu, 2014).

4.2. Simulation and validation

The simulations of urban growth were constrained with the quantities of new urban developments. These quantities were directly acquired from the land-use data (Fig. 2). Figs. 7 and 8 show the simulations and predictions generated by SA-Patch-CA. They were validated using the indicator of 'Figure of merit' (FoM) (Pontius et al., 2007) and landscape metrics to reflect cell-level agreement and pattern-level similarity. The FoM is calculated as follows:

$$F = B/(A + B + C + D) \tag{9}$$

where F is the value of FoM; A is the number of cells that are observed change but simulated as non-change; B is the number of cells that are observed change and simulated as change; C is the number of cells that are observed change and simulated as change but in incorrect gaining category (here C should be set as 0 because SA-Patch-CA only simulates the change of non-urban cells); and D is the number of cells that are observed non-change but simulated as change.

The pattern-level similarity is evaluated using a set of landscape metrics: the number of urban patches (NP), largest-patch index (LPI), mean Euclidean nearest-neighbor distance (ENN) and mean perimeter-area ratio (PARA). They were calculated using FRAGSTATS 4.1 (McGarigal, Cushman, Neel, & Ene, 2012). The pattern-level similarity (a_l) is then calculated as the mean difference of the landscape metrics between the simulated and the observed patterns:

$$a_l = 1 - \frac{1}{8}\sum_i \Delta l_i \tag{8}$$

$$\Delta l_i = \begin{cases} |l_{i,s} - l_{i,o}|/l_{i,o} \times 100\%, l = NP, ENN, PARA \\ |l_{i,s} - l_{i,o}|, l = LPI \end{cases} \tag{9}$$

where $l_{i,s}$ and $l_{i,o}$ represent the ith landscape metric of the simulated and the observed patterns, respectively; and Δl_i is the normalized difference of the ith pair of landscape metrics.

Two recently developed CA models, Logistic-Patch-CA (Chen et al., 2014) and LEI-CA (Liu et al., 2014), were also implemented for a comparative analysis. Logistic-Patch-CA adopts the same patch-based simulation strategy as SA-Patch-CA does, but uses logistic regression to generate the relative weights of explanatory variables. It should be noted that calibration based on logistic regression only involves land-use data at the beginning and the end. This limitation may affect the simulation accuracy of Logistic-Patch-CA as the temporal variations of driving factors cannot be adequately addressed by logistic regression. The inclusion of LEI-CA for comparison is because it shares a similar feature with SA-Patch-CA, i.e. the ability to capture temporal dynamics from empirical land-use data. In LEI-CA, a case-based reasoning (CBR) approach is employed to learn transition knowledge from discrete cases, which are collected and updated from the observed multi-temporal land-use data. This allows LEI-CA to obtain adaptation rules when simulating land-use change in a complex geographical environment.

The validation for all of the three models was first conducted at the cell-level. Fig. 9(a) summarizes the respective proportions of cell-level successes and errors. The indicator of FoM was then calculated based on these proportions. For SA-Patch-CA, the FoM ranges from 0.1366 to 0.2128, which are higher than those of Logistic-Patch-CA (0.1213-0.1920) (Table 5). The higher values of FoM reveals that SA-Patch-CA has a better cell-level accuracy than Logistic-Patch-CA. This is mainly because the approach of SA provides the model with the information of the time-dependent effects in the explanatory variables (Wang et al., 2013). For LEI-CA, however, it yields the highest values of FoM among all of the three

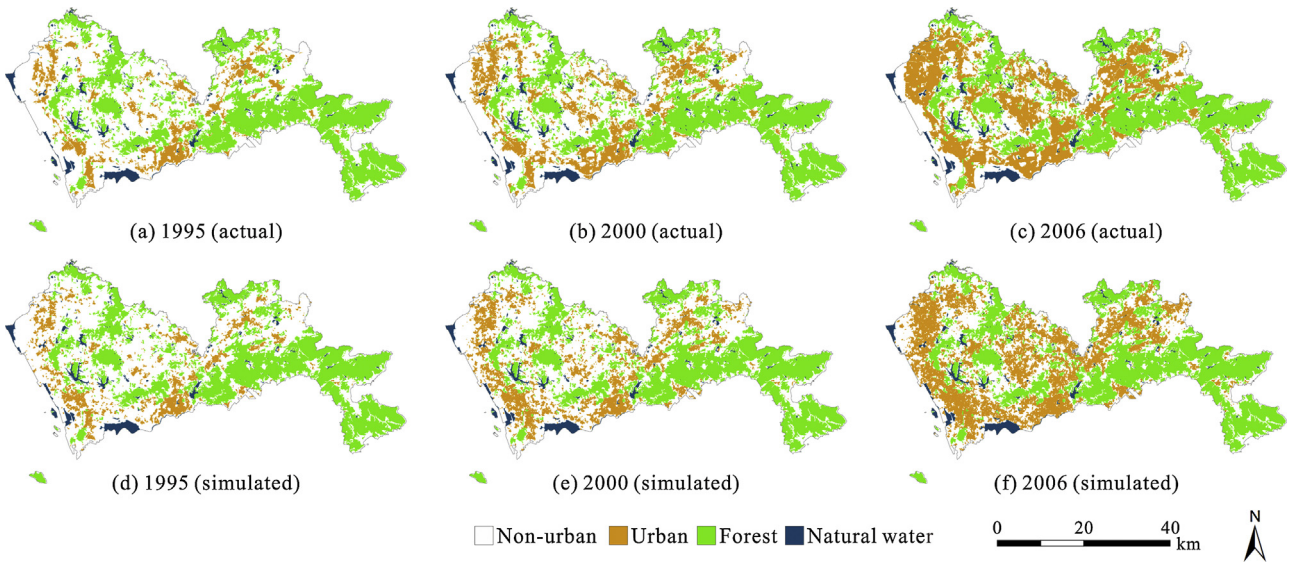

Fig. 7. Simulations of urban land-use patterns in the years of 1995, 2000 and 2006.

Table 5
Comparison of the values of 'Figure of Merit' among SA-Patch-CA, Logistic-Patch-CA and LEI-CA.

Simulation	SA-Patch-CA	Logistic-Patch-CA	LEI-CA
1995	0.1605	0.1356	0.1524
2000	0.1366	0.1213	0.1837
2003	0.2012	0.1730	0.2934
2006	0.1480	0.1294	0.2428
2009	0.1383	0.1219	0.2302
2012	0.2128	0.1920	0.3656

models. This is not surprising because LEI-CA adopts a conventional cell-based simulation strategy which allocates new developed cells more evenly in the space.

Table 6 shows the results of pattern-level similarity. Previous studies have demonstrated that the patch-based simulation strategy can produce results more similar to actual urban development patterns (Chen et al., 2014; García et al., 2012; Meentemeyer et al., 2013). Moreover, the integration of SA can further improve the simulation performance through the effective use of multi-temporal land-use data. According to Table 6, SA-Patch-CA significantly outperforms Logistic-Patch-CA in terms of pattern similarity (81.20% and 69.16%, respectively). One can easily observe from Fig. 10 that the simulation generated by SA-Patch-CA can better match the actual pattern than the one produced by Logistic-Patch-CA. The results also reveal that there are large disagreements between the observed and the simulated values of landscape metrics for LEI-CA. These disagreements are so large that the calculated pattern similarity a_l become invalid. In fact, the patterns generated by LEI-CA are highly fragmented and have a serious "Salt-and-pepper" effect (Figs. Fig. 1010(d) and Fig. 1111). This makes the values of NP extremely large and introduces extra errors to other metrics (Table 6). Overall, the comparative analysis reflects that the proposed SA-Patch-CA has better ability than Logistic-Patch-CA and LEI-CA to replicate realistic urban growth patterns.

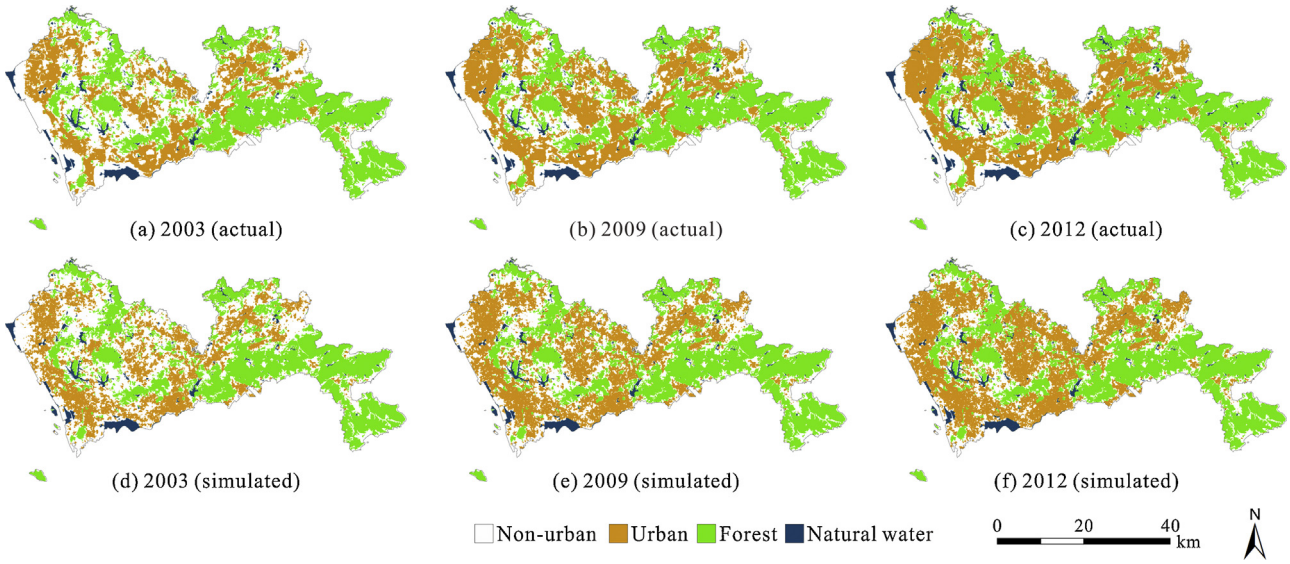

Fig. 8. Predictions of urban land-use patterns in the years of 2003, 2009 and 2012.

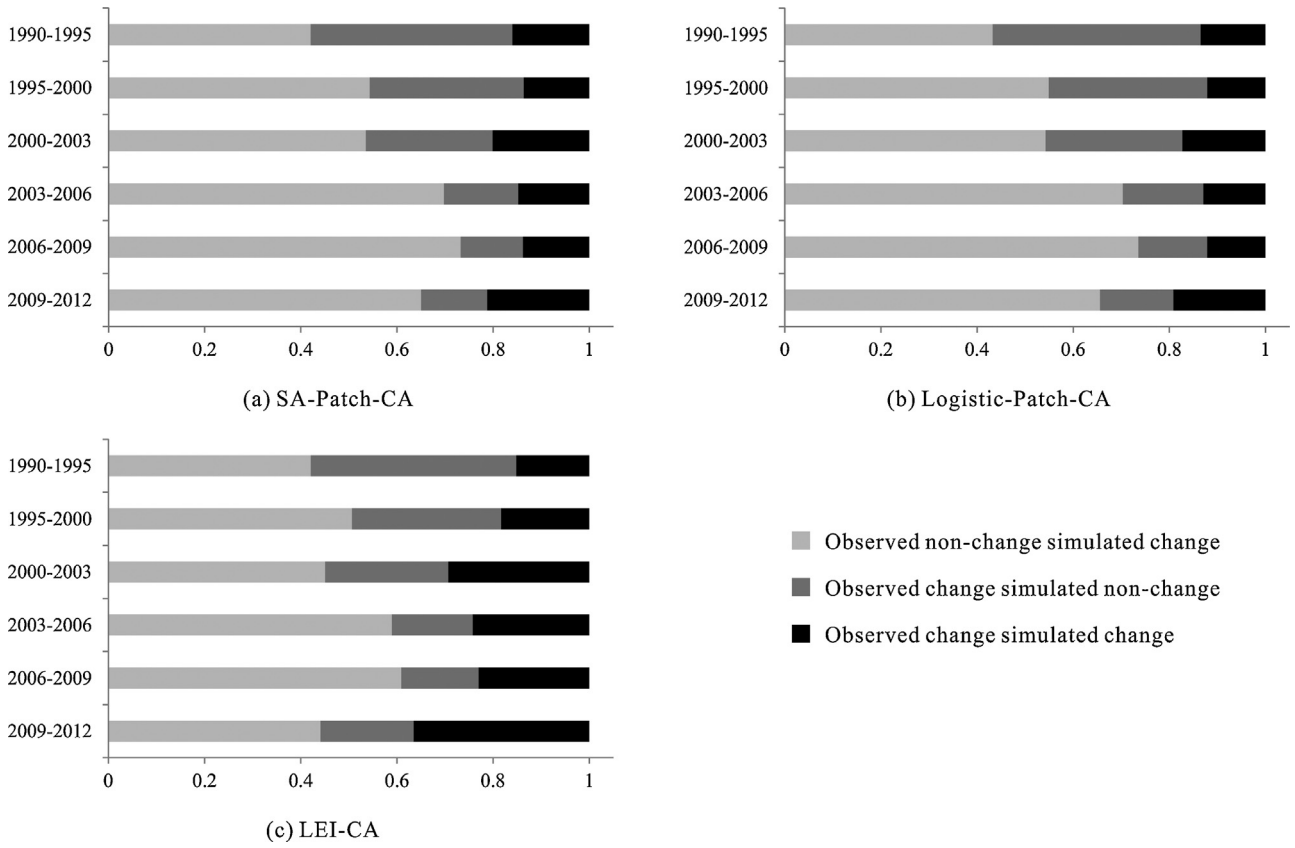

Fig. 9. Quantities of successes and errors for (a) SA-Patch-CA, (b) Logistic-Patch-CA and (c) LEI-CA, respectively.

Table 6
Comparison of observed and simulated values of landscape metrics.

	NP	LPI	ENN	PARA	a_l
1995					
Observed	591	1.80	79.41	101.14	–
Simulated (SA-Patch-CA)	520	1.51	150.02	105.55	73.61%
Simulated (Logistic-Patch-CA)	639	1.89	194.01	111.41	59.33%
Simulated (LEI-CA)	23948	1.46	67.94	447.50	N/A
2000					
Observed	541	3.28	79.37	86.66	–
Simulated (SA-Patch-CA)	580	2.72	113.33	92.15	85.78%
Simulated (Logistic-Patch-CA)	753	2.27	139.48	100.02	67.16%
Simulated (LEI-CA)	15224	2.83	64.92	399.03	N/A
2003					
Observed	522	7.31	70.98	62.62	–
Simulated (SA-Patch-CA)	530	7.93	96.80	78.33	84.10%
Simulated (Logistic-Patch-CA)	652	3.86	109.35	82.59	71.42%
Simulated (LEI-CA)	8460	8.42	61.80	294.74	N/A
2006					
Observed	474	14.02	66.13	52.21	–
Simulated (SA-Patch-CA)	477	17.98	87.08	70.41	84.10%
Simulated (Logistic-Patch-CA)	560	5.41	103.53	73.86	68.81%
Simulated (LEI-CA)	6382	10.69	62.48	228.36	N/A
2009					
Observed	407	15.34	65.28	48.22	–
Simulated (SA-Patch-CA)	467	22.86	81.75	64.61	79.63%
Simulated (Logistic-Patch-CA)	496	7.06	86.45	67.32	74.45%
Simulated (LEI-CA)	5186	11.97	61.21	184.96	N/A
2012					
Observed	567	17.85	63.78	48.48	–
Simulated (SA-Patch-CA)	435	29.84	80.65	57.32	80.00%
Simulated (Logistic-Patch-CA)	415	30.80	89.49	60.73	73.66%
Simulated (LEI-CA)	3976	18.46	61.65	130.47	N/A

4.3. Simulation of development alternatives

The proposed SA-Patch-CA can also be used to simulate future developments under different scenarios. We designed the scenarios based on the diffusion-coalescence theory (Dietzel, Herold, Hemphill, & Clarke, 2005), in which the spatial evolution of a city is described as a two-phase process of diffusion and coalescence. According to this theory, a city starts to grow from its initial seed or core area, and then diffuses to new urban centers (new urban cores). As each of the core areas continue to expand, they begin to coalesce towards each other and might form a new bigger core area (or even a saturated urban landscape). The new core area can be seen as another starting point for a new diffusion-coalescence process, and so on. The diffusion-coalescence process can be measured by using landscape metrics, such as the number of patches (NP). Previous studies reveal that the value of NP increases as urban areas diffuse, and decreases as urban areas coalesce (Dietzel, Oguz, Hemphill, Clarke, & Gazulis, 2005).

In our experiments, new developments of Shenzhen from 2012 to 2018 were simulated under three scenarios: (1) Business-as-usual (BAU). This scenario assumes that Shenzhen follows current development trajectory in the future. (2) Coalescence scenario (COAL). This scenario assumes that the planning agency of the city enhances the spatial connection between new developments and initial urban cores. As a result, the city will form a relatively compact land-use pattern. (3) Diffusion scenario (DIFF). In this scenario, it is assumed that the control of land development will be relaxed in the future. New urban areas might then diffuse in the landscape and result in a fragmented land-use pattern. Table 7 shows the configurations of parameters for each scenario. The parameter T_{spon} in effect constrains the possibility of spontaneous growth in the simulation, and hence it can be used to reflect the top-down control

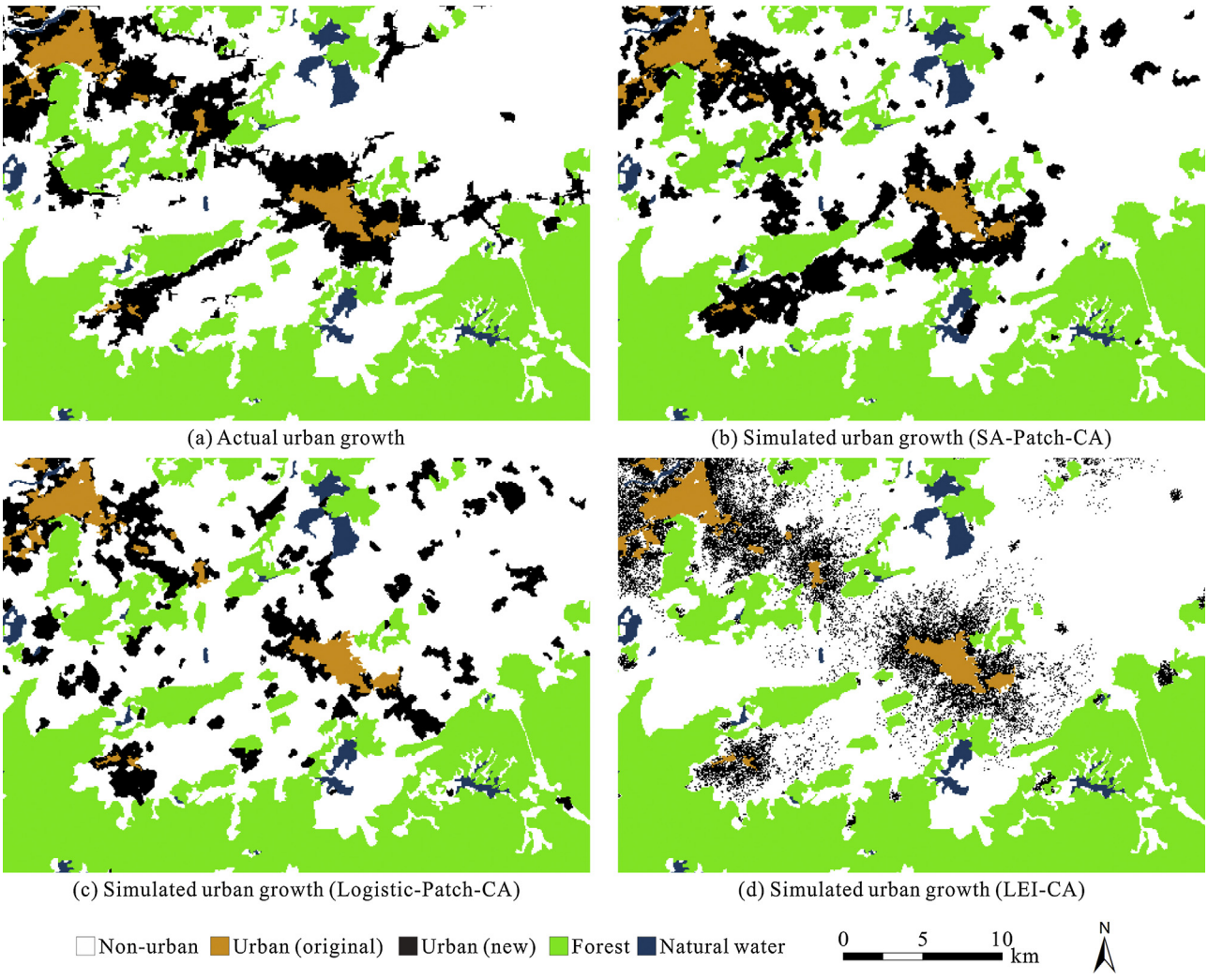

Fig. 10. Comparison of simulated patterns generated by SA-Patch-CA, Logistic-Patch-CA and LEI-CA.

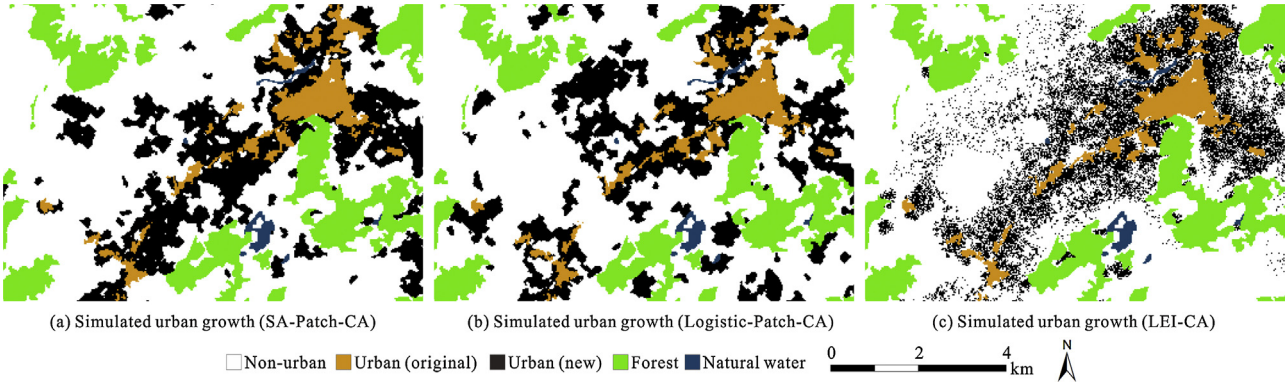

Fig. 11. The "Salt-and-pepper" effect of LEI-CA.

Table 7
Parameter settings of SA-Patch-CA for scenario simulation (2012–2018).

Parameter	a_0	a_1	T_{spon} (BAU)	T_{spon} (COAL)	T_{spon} (DIFF)
Value	12.572	−1.051	0.0057	0.00057	0.057

Note: $a0$ and $a1$ are parameters for calculating Eq. (7); $Tspon$ is the threshold for determining urban growth types (i.e. spontaneous growth or organic growth).

of development tendencies. In the scenario simulations of future development alternatives, because we don't have objective data to rigidly calibrate T_{spon}, we used its past value in 1990–2012 as the baseline (BAU), and enlarged it by 10 times to represent the encouragement of diffusion (DIFF), while reduced it into 1/10 of the baseline value to illustrate the strict regulation of development (COAL).

The results of each scenario are shown in Figs. 12 and 13. In the DIFF scenario, sprawl patterns are witnessed because of the

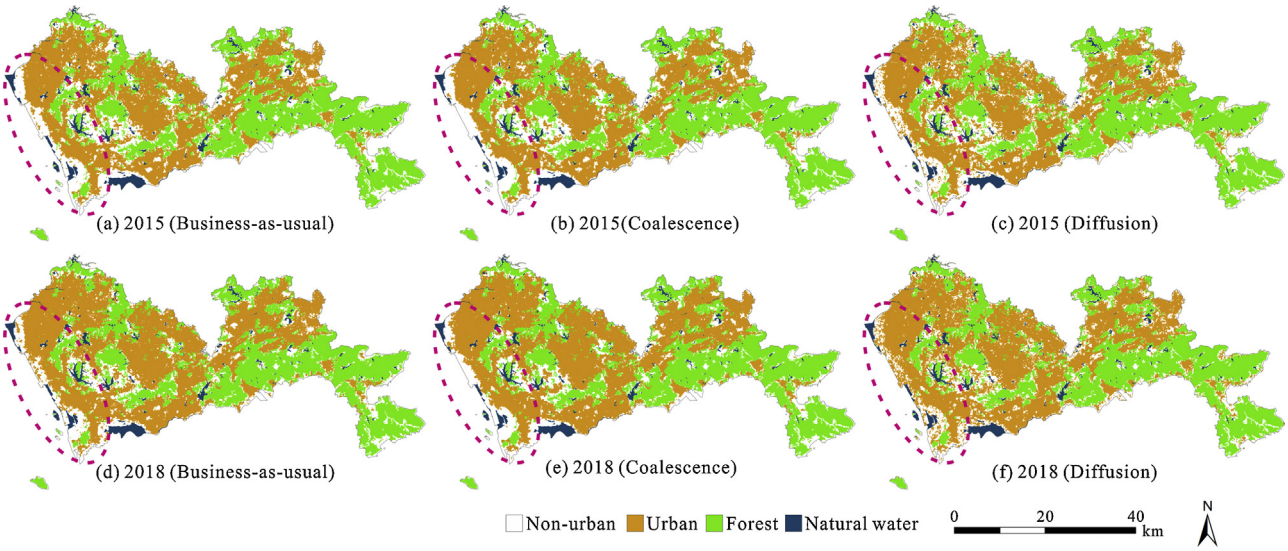

Fig. 12. Scenario simulations of urban expansion in years 2015 and 2018.

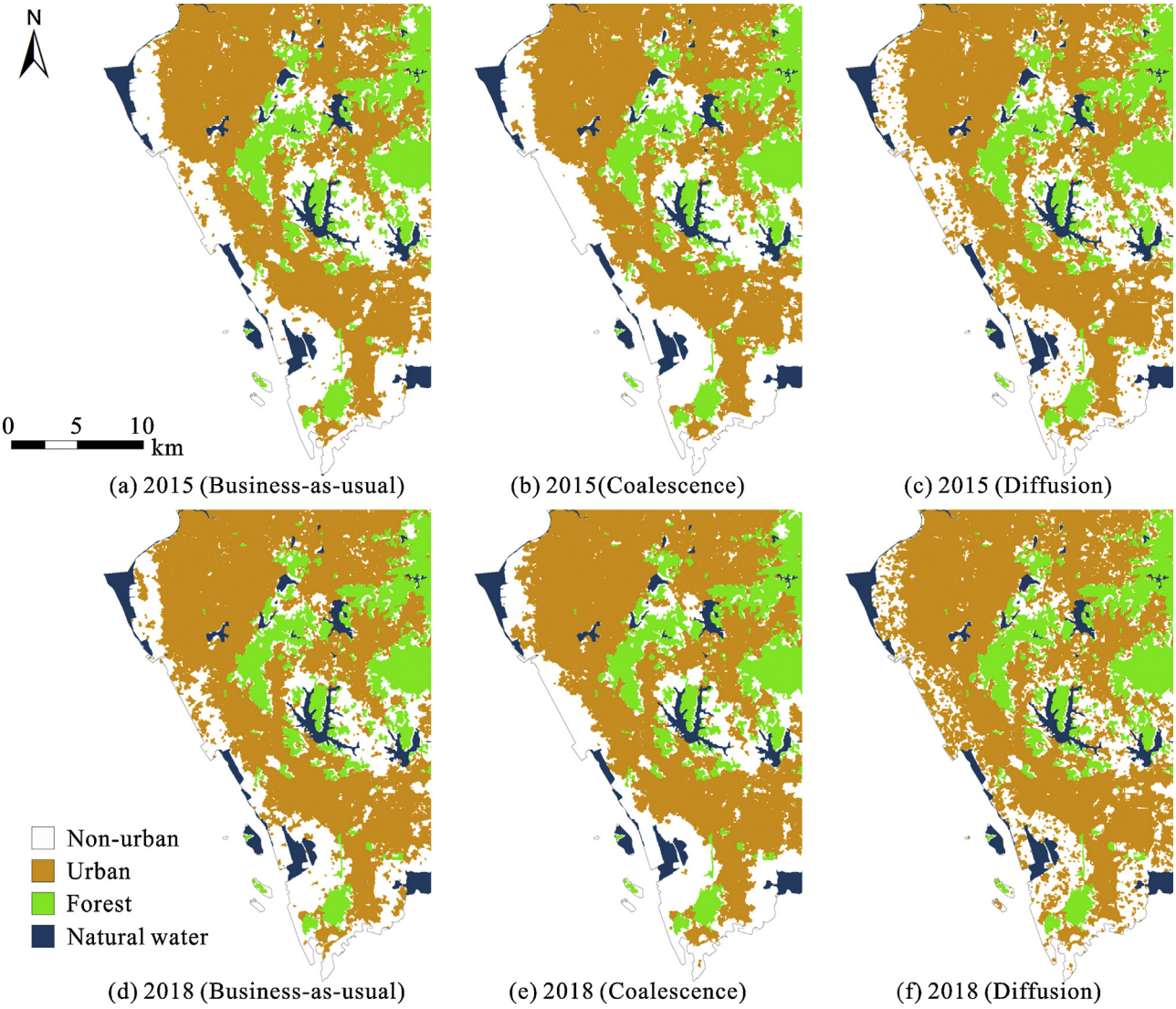

Fig. 13. Simulated land-use patterns in the west coast of Shenzhen under different scenarios.

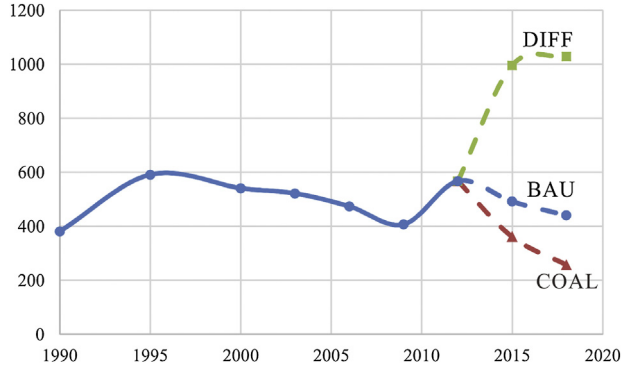

Fig. 14. Simulated values of NP for each scenario.

assumed weak control on development. In the COAL scenario, however, the simulated land-use patterns are less fragmented compared with others in BAU and DIFF scenarios. The metric of NP is calculated for each scenario, and the results are plotted with the historical values of NP to obtain a full phase transition process from 1990 to 2018 (Fig. 14). The changes of NP reveal a clear temporal oscillation between diffusion and coalescence, in which a diffusion phase re-starts in 2009. According to the simulation in BAU scenario, the new started diffusion phase soon turns into a coalescence phase after 2012. The COAL scenario also predicts a phase transition from diffusion to coalescence but with a faster rate. By contrast, the simulation in DIFF scenario suggests that the diffusion phase will even enhance in the next few years. As demonstrated by Figs. 12 and 13, the diffusion of urban areas may occur in the west coast of the city. This is not surprising because there are more vacant spaces for the allocation of new developments, and several planned projects, such as the Binhai New Town and the Qianhai Center (Shenzhen Municipality, 2010), also substantially promote the development potential in this area. Overall, the experimental simulations shown above have demonstrated that SA-Patch-CA can generate various development alternatives as expected.

5. Conclusions

In this study, we aim to improve the performance of CA simulations by utilizing the method of SA to capture the time-dependent influences of driving factors from a time-series of land-use data. In addition, we integrated a patch-based simulation strategy into the model (SA-Patch-CA) to obtain the more realistic urban growth patterns (Chen et al., 2014). The calibrated parameters from SA provide clear signatures of how urban land-use patterns change in Shenzhen (Table 3). It was found that the transportation networks had an intense effect in attracting new developments, and such attraction effect was even increasing over time. A similar result was also identified for the variable of proximity to the port. These findings help explains the formation of the disperse land-use patterns (Fig. 2), which relates to the fast industrialization process in Shenzhen during the past three decades.

The results of our simulation experiments have demonstrated that the proposed SA-Patch-CA significantly outperforms Logistic-Patch-CA with respect to cell- and pattern-level accuracies. This is because the integration of SA allows the more effective use of multi-temporal land-use data. Compared with LEI-CA, the proposed SA-Patch-CA has relatively lower cell-level agreement. This is due to the embedded patch-based simulation strategy that partly reduces the success of prediction at cell-level (Chen et al., 2014). However, SA-Patch-CA avoids the "Salt-and-pepper" effect of LEI-CA and yields more reliable simulations in terms of the similarity to actual land-use patterns. Nevertheless, we will try to improve SA-Patch-CA's cell-level performance in future study. Perhaps extra spatial constraints should be included into the model so that the randomness of the location of simulated patches can be reduced. Moreover, it is crucial to obtain a clearer understanding of the sensitivity of the proposed model to different neighborhood configurations. In this study, we only implemented SA-Patch-CA with the conventional Moore neighborhood (3×3). In the future work, it is worth exploring how the simulation performance changes if various extended neighborhood are applied. It is also necessary to identify the most appropriate neighborhood configuration in order to achieve the best outcomes of SA-Patch-CA for practical uses.

CA models are more and more considered as important operational systems to assist urban planning. SA-Patch-CA also can fulfill this purpose by adjusting the control parameters of the model. In this study, scenario simulation of urban expansion in Shenzhen from 2012 to 2018 was carried out based on SA-Patch-CA. The results suggest that Shenzhen may experience a new coalescence phase from 2012 to 2018 according to the BAU and the COAL scenarios. However, the city is also likely to enhance its diffusion phase if the restriction of land development is relaxed in the future (the DIFF scenario). Overall, the proposed SA-Patch-CA is useful in that it allows urban planners to test, explore and evaluate the outcomes of different planning alternatives. In fact, urban simulation models are frequently coupled with others to address issues relating to urbanization (Clarke, 2014). Thus, our future study may also revolve around the coupling of SA-Patch-CA with other models so that the long term impacts of urban growth can be better predicted and explained.

Acknowledgements

We thank the anonymous reviewers and Prof. Suzana Dragicevic for their valuable comments and suggestions. This research was supported by the Key National Natural Science Foundation of China (Grant No. 41531176), the National Natural Science Foundation of China (Grant No. 41531176), and the Guangdong Natural Science Foundation (Grant No. 2015A030310288).

References

Aljoufie, M., Zuidgeest, M., Brussel, M., van Vliet, J., & van Maarseveen, M. (2013). A cellular automata-based land use and transport interaction model applied to Jeddah, Saudi Arabia. *Landscape and Urban Planning, 112*, 89–99.

Allison, P. D. (2012). *Survival analysis using SAS: a practical guide*. Cary, NC: SAS Institute Inc.

An, L., & Brown, D. G. (2008). Survival analysis in land change science: integrating with GIScience to address temporal complexities. *Annals of the Association of American Geographers, 98*(2), 323–344.

An, L., Brown, D. G., Nassauer, J. I., & Low, B. (2011). Variations in development of exurban residential landscapes: timing, location, and driving forces. *Journal of Land Use Science, 6*(1), 13–32.

Barreira-González, P., Gómez-Delgado, M., & Aguilera-Benavente, F. (2015). From raster to vector cellular automata models: a new approach to simulate urban growth with the help of graph theory. *Computers Environment and Urban Systems, 54*, 119–131.

Basse, R. M., Omrani, H., Charif, O., Gerber, P., & Bódis, K. (2014). Land use changes modelling using advanced methods: cellular automata and artificial neural networks. The spatial and explicit representation of land cover dynamics at the cross-border region scale. *Applied Geography, 53*, 160–171.

Brown, D. G., Page, S., Riolo, R., Zellner, M., & Rand, W. (2005). Path dependence and the validation of agent-based spatial models of land use. *International Journal of Geographical Information Science, 19*(2), 153–174.

Chen, Y., Li, X., Wang, S., Liu, X., & Ai, B. (2013). Simulating urban form and energy consumption in the pearl river delta under different development strategies. *Annals of the Association of American Geographers, 103*(6), 1567–1585.

Chen, Y. M., Li, X., Liu, X. P., & Ai, B. (2014). Modeling urban land-use dynamics in a fast developing city using the modified logistic cellular automaton with a patch-based simulation strategy. *International Journal of Geographical Information Science, 28*(2), 234–255.

Clarke, K., & Gaydos, L. (1998). Loose-coupling a cellular automaton model and GIS: long-term urban growth prediction for San Francisco and Washington/Baltimore. *International Journal of Geographical Information Science, 12*(7), 699–714.

Clarke, K. C. (2014). Why simulate cities? *GeoJournal, 79*(2), 129–136.

Cox, D. R. (1972). Regression models and life-tables. *Journal of the Royal Statistical Society. Series B (Methodological)*, 187–220.
Dietzel, C., Herold, M., Hemphill, J. J., & Clarke, K. C. (2005). Spatio-temporal dynamics in California's Central Valley: empirical links to urban theory. *International Journal of Geographical Information Science*, *19*(2), 175–195.
Dietzel, C., Oguz, H., Hemphill, J., Clarke, K., & Gazulis, N. (2005). Diffusion and coalescence of the Houston metropolitan area: evidence supporting a new urban theory. *Environment and Planning B: Planning and Design*, *32*(2), 231–246.
Fragkias, M., & Seto, K. (2009). Evolving rank-size distributions of intra-metropolitan urban clusters in South China. *Computers, Environment and Urban Systems*, *33*(3), 189–199.
Güneralp, B., & Seto, K. C. (2008). Environmental impacts of urban growth from an integrated dynamic perspective: a case study of Shenzhen, South China. *Global Environmental Change*, *18*(4), 720–735.
García, A. M., Santé, I., Boullón, M., & Crecente, R. (2012). A comparative analysis of cellular automata models for simulation of small urban areas in Galicia, NW, Spain, *Computers. Environment and Urban Systems*, *36*(4), 291–301.
Greenberg, J. A., Kefauver, S. C., Stimson, H. C., Yeaton, C. J., & Ustin, S. L. (2005). Survival analysis of a neotropical rainforest using multitemporal satellite imagery. *Remote Sensing of Environment*, *96*(2), 202–211.
He, C., Zhao, Y., Tian, J., & Shi, P. (2013). Modeling the urban landscape dynamics in a megalopolitan cluster area by incorporating a gravitational field model with cellular automata. *Landscape and Urban Planning*, *113*, 78–89.
Hou, Q., & Li, S. (2011). Transport infrastructure development and changing spatial accessibility in the Greater Pearl River Delta, China 1990–2020. *Journal of Transport Geography*, *19*(6), 1350–1360.
Kocabas, V., & Dragicevic, S. (2006). Assessing cellular automata model behaviour using a sensitivity analysis approach. *Computers Environment and Urban Systems*, *30*(6), 921–953.
Li, X., & Yeh, A. G. O. (2002). Neural-network-based cellular automata for simulating multiple land use changes using GIS. *International Journal of Geographical Information Science*, *16*(4), 323–343.
Li, X., & Yeh, A. G. O. (2004). Data mining of cellular automata's transition rules. *International Journal of Geographical Information Science*, *18*(8), 723–744.
Liu, X. P., Li, X., Liu, L., He, J., & Ai, B. (2008). A bottom-up approach to discover transition rules of cellular automata using ant intelligence. *International Journal of Geographical Information Science*, *22*(11–12), 1247–1269.
Liu, X., Li, X., Chen, Y., Tan, Z., Li, S., & Ai, B. (2010). A new landscape index for quantifying urban expansion using multi-temporal remotely sensed data. *Landscape Ecology*, *25*(5), 671–682.
Liu, X. P., Ma, L., Li, X., Ai, B., Li, S. Y., & He, Z. J. (2014). Simulating urban growth by integrating landscape expansion index (LEI) and cellular automata. *International Journal of Geographical Information Science*, *28*(1), 148–163.
McGarigal, K., Cushman, S., Neel, M., & Ene, E. (2012). *FRAGSTATS v4: spatial pattern analysis program for categorical and continuous maps*. Amherst: Computer software program produced by the authors at the University of Massachusetts.
Meentemeyer, R. K., Tang, W., Dorning, M. A., Vogler, J. B., Cunniffe, N. J., & Shoemaker, D. A. (2013). FUTURES: multilevel simulations of emerging urban–rural landscape structure using a stochastic patch-Growing algorithm. *Annals of the Association of American Geographers*, *103*(4), 785–807.
Moreno, N., Ménard, A., & Marceau, D. J. (2008). VecGCA: a vector-based geographic cellular automata model allowing geometric transformations of objects. *Environment and Planning B: Planning and Design*, *35*(4), 647–665.
Moreno, N., Wang, F., & Marceau, D. J. (2009). Implementation of a dynamic neighborhood in a land-use vector-based cellular automata model. *Computers, Environment and Urban Systems*, *33*(1), 44–54.
Ng, M. K. (2003). Shenzhen. *Cities*, *20*(6), 429–441.
Ng, M. K., & Xu, J. (2014). Second metamorphosis? urban restructuring and planning responses in guangzhou and shenzhen in the twenty-first century. In *Maturing megacities*. pp. 29–60. Springer.
Omrani, H., Abdallah, F., Charif, O., & Longford, N. T. (2015). Multi-label class assignment in land-use modelling. *International Journal of Geographical Information Science*, *29*(6), 1023–1041.
Pontius, R., Walker, R., Yao-Kumah, R., Arima, E., Aldrich, S., Caldas, M., et al. (2007). Accuracy assessment for a simulation model of Amazonian deforestation. *Annals of the Association of American Geographers*, *97*(4), 677–695.
Samardžić-Petrović, M., Dragićević, S., Kovačević, M., & Bajat, B. (2015). Modeling urban land use changes using support vector machines. *Transactions in GIS* (in press)
Santé, I., García, A., Miranda, D., & Crecente, R. (2010). Cellular automata models for the simulation of real-world urban processes: a review and analysis. *Landscape and Urban Planning*, *96*(2), 108–122.
Seto, K. C., Fragkias, M., Güneralp, B., & Reilly, M. K. (2011). A meta-analysis of global urban land expansion. *PLoS*, *6*(8), e23777.
Seto, K. C., Woodcock, C. E., Song, C., Huang, X., Lu, J., & Kaufmann, R. K. (2002). Monitoring land-use change in the pearl river delta using landsat TM. *International Journal of Remote Sensing*, *23*(10), 1985–2004.
Shenzhen Municipality, 2010, *The Comprehensive Plan of Shenzhen City 2010–2020*, http://www.szpl.gov.cn/xxgk/csgh/csztgh/201009/t20100929_60694.htm (accessed 01.04.16.).
Shin, H. B. (2014). Urban spatial restructuring, event-led development and scalar politics. *Urban Studies*, *51*(14), 2961–2978.
Stevens, D., Dragicevic, S., & Rothley, K. (2007). iCity: a GIS–CA modelling tool for urban planning and decision making. *Environmental Modelling & Software*, *22*(6), 761–773.
Sui, D., & Zeng, H. (2001). Modeling the dynamics of landscape structure in Asia's emerging desakota regions: a case study in Shenzhen. *Landscape and Urban Planning*, *53*(1–4), 37–52.
Tayyebi, A., & Pijanowski, B. C. (2014). Modeling multiple land use changes using ANN, CART and MARS: Comparing tradeoffs in goodness of fit and explanatory power of data mining tools. *International Journal of Applied Earth Observation and Geoinformation*, *28*, 102–116.
Wang, F., & Marceau, D. J. (2013). A patch-based cellular automaton for simulating land-use changes at fine spatial resolution. *Transactions in GIS*, *17*(6), 828–846.
Wang, N., Brown, D. G., An, L., Yang, S., & Ligmann-Zielinska, A. (2013). Comparative performance of logistic regression and survival analysis for detecting spatial predictors of land-use change. *International Journal of Geographical Information Science*, *27*(10), 1960–1982.
Wu, F. (2002). Calibration of stochastic cellular automata: the application to rural-urban land conversions. *International Journal of Geographical Information Science*, *16*(8), 795–818.